Extracting Nucleon Strange and Anapole Form Factors from World Data

R. D. Young,[1] J. Roche,[1,2] R. D. Carlini,[1] and A. W. Thomas[1]

[1]*Jefferson Lab, 12000 Jefferson Avenue, Newport News, Virginia 23606, USA*
[2]*Rutgers, The State University of New Jersey, Piscataway, New Jersey 08854, USA*

The complete world set of parity-violating electron scattering data up to $Q^2 \sim 0.3$ GeV^2 is analyzed. We extract the current experimental determination of the strange electric and magnetic form factors of the proton, as well as the weak axial form factors of the proton and neutron, at $Q^2 = 0.1$ GeV^2. Within experimental uncertainties, we find that the strange form factors are consistent with zero, as are the anapole contributions to the axial form factors. Nevertheless, the correlation between the strange and anapole contributions suggest that there is only a small probability that these form factors all vanish simultaneously.

Parity-violating electron scattering (PVES) is an essential tool in mapping out the flavor composition of the electromagnetic form factors. Exposing the role of the strange quark via these measurements provides direct information on the underlying dynamics of nonperturbative QCD—a considerable achievement both experimentally and theoretically. The most precise separation of the strange electric and magnetic form factors is available at $Q^2 \simeq 0.1$ GeV^2, where experiments by the SAMPLE [1,2], PVA4 [3], and HAPPEx [4,5] collaborations have been performed with varying kinematics and targets. At higher Q^2, HAPPEx [6,7], PVA4 [8], and the forward angle G0 experiment [9] provide further information over the range $Q^2 \sim 0.12$–1.0 GeV^2. Here we use systematic expansions of all the unknown form factors to simultaneously analyze the current data set and extract the values at $Q^2 = 0.1$ GeV^2, independent of theoretical input—other than the constraint of charge symmetry. The results provide a critical test of modern theoretical estimates of the anapole moment of the proton and neutron as well as their strange form factors.

The proton-PVES experiments are sensitive to the strange form factors G_E^s and G_M^s, and the electroweak axial form factor $\tilde{G}_A^p$—which includes the anapole form factor [10,11]. Previously, limited experimental data made it difficult to carry out a simultaneous separation of all three form factors; instead, assumptions were made on the (in)significance of certain contributions based on the kinematic domain and/or the use of theoretical calculations. In combining proton and deuteron data, there are two independent anapole form factors. Together with the two strange form factors, this analysis presents the first extraction of all four form factors from data. No more than two independent terms have been fit simultaneously in any previous analysis. Further, no analysis has attempted to determine the isoscalar anapole term from data. This contribution is quite poorly constrained by experiment and the design of an appropriate measurement to improve this situation is both a theoretical and experimental challenge.

The role of the strange quark is probed by measuring the PV asymmetry in polarized e-N scattering, for which the dominant contribution arises from interference between the γ and Z^0 exchange. The majority of measurements have been performed on hydrogen: SAMPLE [2,12], HAPPEx [5,6], PVA4 [3,8], and G0 [9].

As described in Ref. [13], the PV asymmetry for a proton target is given by (assuming charge symmetry)

$$A_{LR}^p = \frac{d\sigma_R - d\sigma_L}{d\sigma_R + d\sigma_L} = -\frac{G_\mu Q^2}{4\pi\alpha\sqrt{2}}\frac{A_V^p + A_s^p + A_A^p}{\epsilon G_E^p + \tau G_M^p}, \quad (1)$$

$$A_V^p = \xi_V^p(\epsilon G_E^p + \tau G_M^p) + \xi_V^n(\epsilon G_E^p G_E^n + \tau G_M^p G_M^n), \quad (2)$$

$$A_s^p = \epsilon G_E^p \xi_V^0 G_E^s + \tau G_M^p \xi_V^0 G_M^s, \quad (3)$$

$$A_A^p = -(1 - 4\hat{s}^2)\sqrt{1 - \epsilon^2}\sqrt{\tau(1 + \tau)}G_M^p\tilde{G}_A^p. \quad (4)$$

The kinematic variables are defined by $\epsilon \equiv [1 + 2(1 + \tau)\tan^2\theta/2]^{-1}$ and $\tau \equiv |Q^2|/4M_p^2$. The standard model parameters α, G_μ, and $\hat{s}^2 \equiv \sin^2\hat{\theta}_W$ are taken from the PDG [14]. The vector radiative correction factors are defined by $\xi_V^p = (1 - 4\hat{s}^2)(1 + R_V^p)$, $\xi_V^n = -(1 + R_V^n)$, and $\xi_V^0 = -(1 + R_V^{(0)})$, with $R_V^p = -0.04471$ and $R_V^n = R_V^{(0)} = -0.01179$ [14]. The axial radiative and anapole corrections remain implicit in $\tilde{G}_A^p$, as this entire contribution is to be fit to data.

Scattering from targets other than the proton provides access to different flavor components of the nucleon form factors. The HAPPEx Collaboration have recently utilized a helium-4 target to directly extract the strange electric form factor [4], where the theoretical asymmetry can be written as

$$A_{LR}^{\text{He}} = \frac{G_\mu Q^2}{4\pi\alpha\sqrt{2}}\left[(\xi_V^p + \xi_V^n) + 2\frac{\xi_V^0 G_E^s}{G_E^p + G_E^n}\right]. \quad (5)$$

In the SAMPLE experiment, which detected electrons scattered at backward angles, the contribution from G_E^s is

substantially suppressed. These measurements were primarily sensitive to a linear combination of the axial and strange magnetic form factors. In addition to the proton target, the PV asymmetry has also been measured on the deuteron [1]. While providing a different combination of G_M^s and $\tilde{G}_A^p$, this also introduces sensitivity to the neutron axial form factor.

Scattering from the deuteron is dominated by the quasielastic interaction with the nucleon constituents. The analysis of the deuteron results [12] has also included nuclear corrections, involving a realistic deuteron wave function, rescattering effects, and the small contribution from elastic deuteron scattering [15]. Further parity-violating contributions arising from the deuteron wave function and exchange currents, while small [15], have been included.

A combined analysis of the current world PV data requires a consistent treatment of the vector and axial form factors and radiative corrections. Our theoretical asymmetries have therefore been reconstructed for each measurement. The theoretical asymmetry is

$$A_{PV}^{\text{theory}} = \eta_0 + \eta_A^p \tilde{G}_A^p + \eta_A^n \tilde{G}_A^n + \eta_E G_E^s + \eta_M G_M^s, \quad (6)$$

where the values of η_i, given in Table I, include the latest vector form factors [16] and PDG radiative corrections.

It has been observed that the strange form factors are mildly sensitive to the choice of form factor parametrization, with an uncertainty dominated by the neutron charge form factor. To test the sensitivity to G_E^n, we explicitly included the experimental data for G_E^n [17] in our global fit. Over the low-Q^2 domain required in this analysis, the form factor can be parametrized by a Taylor expansion up to $\mathcal{O}(Q^6)$. This made no significant difference to the final extraction, and hence the central value of the Kelly parametrization [16] is taken in the following analysis.

In order to extract all three form factors using as much data as possible, we parametrize their Q^2 dependence. At low momentum transfer, a Taylor series expansion in Q^2 is sufficient and minimizes the model dependence of the determined form factors. The quality of a Taylor series expansion can be estimated phenomenologically. Vector meson dominance would suggest that the Q^2 evolution of the form factors be no more rapid than a dipole with mass parameter $\sim m_\phi \sim 1$ GeV. Similarly, lattice QCD simulations in the vicinity of the strange quark yield behavior consistent with a dipole of scale >1 GeV [18,19]. With the aim of fitting data up to $Q^2 \sim 0.3$ GeV^2, approximating a dipole by a constant over this range would lead to less than 20% uncertainty (less than 10% at the next order in Q^2).

TABLE I. Displayed are the η_i, appearing in Eq. (6), which describe the theoretical asymmetry for each experiment (in parts per million). The measured asymmetry is shown by A^{phys} and the corresponding uncertainty, δA, where sources of error have been added in quadrature. The second uncertainty, δA_{cor}, represents the correlated error in the G0 experiment [9]. Columns on the right show the determination of the form factors at $Q^2 = 0.1$ GeV^2 for fits which include all data up to the given measurement (statistical uncertainty on final decimal place shown in parentheses). The reduced χ^2 for each fit is displayed, followed in the final column by the confidence level (C.L.) for the true value of the strangeness form factors to be nonzero.

Collaboration	Q^2	η_0	η_A^p	η_A^n	η_E	η_M	A^{phys}	δA	δA_{cor}	$\tilde{G}_A^p$	$\tilde{G}_A^n$	G_E^s	G_M^s	χ^2	C.L.
SAMPLE	0.038	−2.13	0.46	−0.30	1.16	0.28	−3.51	0.81	0	⋯	⋯	⋯	⋯	⋯	
SAMPLE	0.091	−7.02	1.04	−0.65	1.63	0.77	−7.77	1.03	0	⋯	⋯	⋯	⋯	⋯	
HAPPEx	0.091	−7.50	0	0	−20.2	0	−6.72	0.87	0	⋯	⋯	⋯	⋯	⋯	
HAPPEx	0.099	−1.40	0.04	0	9.55	0.76	−1.14	0.25	0	⋯	⋯	⋯	⋯	⋯	
SAMPLE	0.1	−5.47	1.58	0	2.11	3.46	−5.61	1.11	0	−2.6(21)	−0.6(30)	−0.044(47)	1.00(75)	1.0	63
PVA4	0.108	−1.80	0.26	0	10.1	1.05	−1.36	0.32	0	−2.0(20)	0.3(29)	−0.025(43)	0.87(74)	1.0	71
G0	0.122	−1.90	0.06	0	12.0	1.18	−1.51	0.49	0.18	−1.8(19)	0.5(27)	−0.023(43)	0.79(69)	0.7	76
G0	0.128	−2.04	0.06	0	12.6	1.30	−0.97	0.46	0.17	−2.4(18)	−0.1(26)	−0.027(42)	0.99(65)	0.7	96
G0	0.136	−2.24	0.07	0	13.5	1.48	−1.30	0.45	0.17	−2.5(17)	−0.2(26)	−0.028(42)	1.03(63)	0.6	99
G0	0.144	−2.44	0.08	0	14.3	1.67	−2.71	0.47	0.18	−1.6(16)	0.8(25)	−0.021(42)	0.71(61)	1.4	91
G0	0.153	−2.68	0.09	0	15.3	1.89	−2.22	0.51	0.21	−1.4(16)	1.0(25)	−0.020(42)	0.66(60)	1.2	91
G0	0.164	−2.97	0.11	0	16.5	2.19	−2.88	0.54	0.23	−1.1(16)	1.3(25)	−0.018(42)	0.55(60)	1.2	83
G0	0.177	−3.34	0.13	0	18.0	2.58	−3.95	0.50	0.20	−0.4(16)	2.1(24)	−0.012(42)	0.32(59)	1.7	36
G0	0.192	−3.78	0.15	0	19.7	3.07	−3.85	0.53	0.19	−0.2(15)	2.3(24)	−0.010(42)	0.24(58)	1.6	18
G0	0.210	−4.34	0.19	0	21.8	3.72	−4.68	0.54	0.21	0.1(15)	2.7(24)	−0.007(42)	0.14(57)	1.6	1
PVA4	0.230	−5.66	0.89	0	22.6	5.07	−5.44	0.60	0	0.0(15)	2.5(24)	−0.007(42)	0.14(57)	1.5	1
G0	0.232	−5.07	0.23	0	24.4	4.61	−5.27	0.59	0.23	0.2(14)	2.8(23)	−0.005(42)	0.09(57)	1.4	3
G0	0.262	−6.12	0.31	0	28.0	5.99	−5.26	0.53	0.17	−0.2(14)	2.3(23)	−0.010(41)	0.19(56)	1.4	18
G0	0.299	−7.51	0.42	0	32.6	8.00	−7.72	0.80	0.35	0.0(14)	2.6(23)	−0.006(41)	0.12(55)	1.3	5
G0	0.344	−9.35	0.57	0	38.4	10.9	−8.40	1.09	0.52	0.0(14)	2.5(22)	−0.008(41)	0.15(54)	1.2	11
G0	0.410	−12.28	0.87	0	47.3	16.1	−10.25	1.11	0.55	−0.4(13)	2.1(22)	−0.015(40)	0.27(53)	1.2	44
HAPPEx	0.477	−15.46	1.12	0	56.9	22.6	−15.05	1.13	0	0.1(12)	2.7(21)	−0.004(38)	0.10(49)	1.2	28

To isolate the individual form factors at higher-Q^2, a combination of neutrino and parity-violating electron scattering should provide the tightest constraint, as described in Ref. [20].

We describe the Q^2 dependence of the form factors over the range $0 < Q^2 < 0.3$ GeV^2 by

$$\tilde{G}_A^N = \tilde{g}_A^N (1 + Q^2/M_A^2)^{-2}, \qquad (7)$$

$$G_E^s = \rho_s Q^2 + \rho_s' Q^4, \qquad G_M^s = \mu_s + \mu_s' Q^2. \qquad (8)$$

The momentum dependence of the radiative corrections is assumed to be mild, and therefore the axial dipole mass is chosen to be that determined from neutrino scattering, $M_A = 1.026$ GeV [21].

The best fit for $Q^2 < 0.3$ GeV^2 yields, at leading order in Q^2, a reduced $\chi^2 = 19.7/15 = 1.3$, with parameters

$$\tilde{g}_A^p = 0.05 \pm 1.38 \mp 0.29, \qquad (9)$$

$$\tilde{g}_A^n = 2.61 \pm 2.27 \mp 0.37, \qquad (10)$$

$$\rho_s = -0.06 \pm 0.41 \mp 0.00 \text{ GeV}^{-2}, \qquad (11)$$

$$\mu_s = 0.12 \pm 0.55 \pm 0.07. \qquad (12)$$

The second error bar displays the sensitivity to the correlated error in the G0 experiment, where the data have been refit using $A^{\text{phys}} \pm \delta A_{\text{cor}}$. The extraction of the strange form factors over the low-Q^2 range is shown in Fig. 1. We display the joint determination of the strange electric and magnetic form factors at $Q^2 = 0.1$ GeV^2 in Fig. 2, where we also show the theoretical calculations of Leinweber *et al.* [22,23]. Similar contours in $\tilde{G}_A^p - G_M^s$ and $\tilde{G}_A^p - \tilde{G}_A^n$ space are shown in Fig. 3.
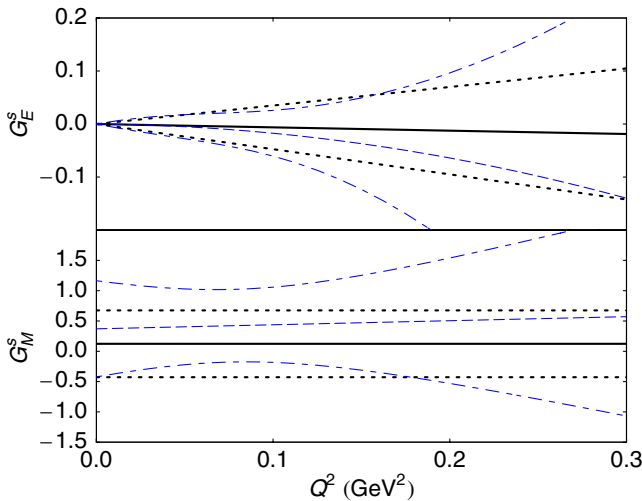
The stability of the fits to truncation of the data set at a maximum Q^2 value has been investigated. The resulting fits are displayed in Table I, where a clear signal for nonzero strangeness is observed in the vicinity of $Q^2 \sim 0.1$ GeV^2—with caution that the fits are particularly sensitive to truncation up until $Q^2 \sim 0.2$ GeV^2. To investigate a potential enhancement near $Q^2 \sim 0.1$ GeV^2, we include the second-order terms of Eq. (8) and fit all data for $Q^2 < 0.3$ GeV^2. This produces a $\chi^2 = 18.1/13 = 1.4$ and best-fit parameters $\tilde{g}_A^p = -0.80 \pm 1.68$, $\tilde{g}_A^n = 1.65 \pm 2.62$, $\rho_s = -0.03 \pm 0.63$ GeV^{-2}, $\rho_s' = -1.5 \pm 5.8$ GeV^{-4}, $\mu_s = 0.37 \pm 0.79$, and $\mu_s' = 0.7 \pm 6.8$ GeV^{-2}, where the errors are statistical only. Figure 1 shows the uncorrelated separation of the electric and magnetic form factors at this order. Where the data are best constrained, $Q^2 \sim 0.1$ GeV^2, there is only a 55% C.L. in support of nonzero strangeness. This suggests that the strangeness signal in Table I, obtained by truncating the data at $Q^2 \sim 0.14$ GeV^2, is consistent with a random fluctuation.

Previous (nonglobal) attempts to extract the nucleon strange form factors from world data used a theoretical prediction of $\tilde{g}_A^N$ [11]. In the following, we compare the axial form factors extracted from the data with this prediction. We write the axial charges, Eq. (7), as

$$\tilde{g}_A^N = \xi_A^{T=1} G_A \tau_3 + \xi_A^{T=0} a_8 + \xi_A^0 a_s + A_{\text{ana}}^N, \qquad (13)$$

with $\tau_3 = 1(-1)$ for the proton (neutron). The radiative corrections are implied to be single-quark only $\xi_A^{T=1} = -0.828$, $\xi_A^{T=0} = -0.126$, and $\xi_A^0 = 0.449$ [14]. The axial charges are relatively well known, where we use
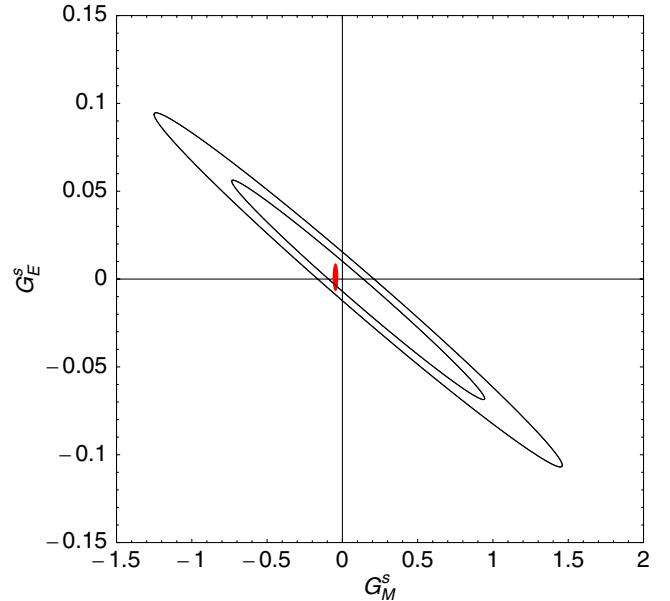

FIG. 1 (color online). The strange electric and magnetic form factors. The solid curve shows the leading-order fit, with 1-σ bound shown by the dotted curves. The dashed and dash-dotted curves show the fit and error of the next-to-leading-order fit.

FIG. 2 (color online). The contours display the 68% and 95% confidence intervals for the joint determination of G_M^s and G_E^s at $Q^2 = 0.1$ GeV^2. The solid ellipse shows the theoretical results of Leinweber *et al.* [22,23].
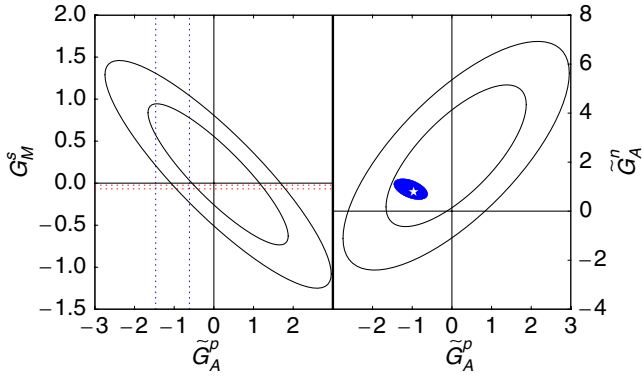
FIG. 3 (color online). The contours display the 68% and 95% confidence intervals for the joint determination of the form factors (defined on the axes) at $Q^2 = 0.1$ GeV^2. The horizontal and vertical bands in the left panel show the theory results of Leinweber et al. [22] and Zhu et al. [11], respectively. The disk in the right panel displays the theoretical result of Zhu et al. [11], with the white star indicating the zero anapole origin. [The same dipole behavior as Eq. (7) is assumed.]

$G_A = 1.2695$, $a_8 = 0.58 \pm 0.03 \pm 0.12$ [24] and $a_s = -0.07 \pm 0.04 \mp 0.05$ [25]. The second error in a_8 and a_s reflects estimates of the SU(3)-flavor symmetry violations of ~20% in the determination of a_8 from hyperon β decay [26]. The dominant source of uncertainty in Eq. (13) is the anapole contribution, $A_{ana}^N = A_{ana}^{(T=1)} \tau_3 + A_{ana}^{(T=0)}$. Converting the result of Zhu et al. [11] to $\overline{MS}$ [27], the anapole terms are estimated to be $A_{ana}^{(T=1)} = -0.11 \pm 0.44$ and $A_{ana}^{(T=0)} = 0.02 \pm 0.26$. This gives the total theory estimates for the axial charges in PVES, $\tilde{G}_A^p = (-1.16 \pm 0.04) + (-0.09 \pm 0.51)$ and $\tilde{G}_A^n = (0.95 \pm 0.04) + (0.13 \pm 0.51)$, where the second term is the anapole contribution. These estimates are consistent with the present determination, as shown in the right panel of Fig. 3.

As we see from Table I, the current world data are consistent with the strange form factors being zero at a high level of confidence. The anapole contributions, considered alone, are also consistent with zero. On the other hand, if one interrogates the data for the probability that strange and anapole form factors are simultaneously zero, within the current errors, the hypothesis is only supported at 8%. While the present data set cannot distinguish the origin of this effect, there appears to be significant support for a nonzero signal in at least one of the strange or anapole contributions.

In conclusion, our analysis of the world data set for PVES has yielded the best experimental determination, at low Q^2, of the strange electric and magnetic form factors of the proton as well as the anapole form factors of the proton and neutron. While both the strangeness and anapole contributions are consistent with zero, we expect that the

additional HAPPEx and G0-backward angle experiments at Jefferson Lab and the PVA4-backward angle experiment at Mainz will soon yield data that, when combined with this analysis, could reveal a nontrivial result for at least one of these form factors.

[1] T. M. Ito et al. (SAMPLE Collaboration), Phys. Rev. Lett. **92**, 102003 (2004).
[2] D. T. Spayde et al. (SAMPLE Collaboration), Phys. Lett. B **583**, 79 (2004).
[3] F. E. Maas et al., Phys. Rev. Lett. **94**, 152001 (2005).
[4] K. A. Aniol et al. (HAPPEX Collaboration), Phys. Rev. Lett. **96**, 022003 (2006).
[5] K. A. Aniol et al. (HAPPEX Collaboration), Phys. Lett. B **635**, 275 (2006).
[6] K. A. Aniol et al. (HAPPEX Collaboration), Phys. Lett. B **509**, 211 (2001).
[7] K. A. Aniol et al. (HAPPEX Collaboration), Phys. Rev. C **69**, 065501 (2004).
[8] F. E. Maas et al. (A4 Collaboration), Phys. Rev. Lett. **93**, 022002 (2004).
[9] D. S. Armstrong et al. (G0 Collaboration), Phys. Rev. Lett. **95**, 092001 (2005).
[10] M. J. Musolf and B. R. Holstein, Phys. Lett. B **242**, 461 (1990).
[11] S. L. Zhu et al., Phys. Rev. D **62**, 033008 (2000).
[12] E. J. Beise, M. L. Pitt, and D. T. Spayde, Prog. Part. Nucl. Phys. **54**, 289 (2005).
[13] M. J. Musolf et al., Phys. Rep. **239**, 1 (1994).
[14] S. Eidelman et al. (PDG), Phys. Lett. B **592**, 1 (2004).
[15] R. Schiavilla et al., Phys. Rev. C **70**, 044007 (2004); **67**, 032501 (2003).
[16] J. J. Kelly, Phys. Rev. C **70**, 068202 (2004).
[17] C. E. Hyde-Wright and K. de Jager, Annu. Rev. Nucl. Part. Sci. **54**, 217 (2004).
[18] M. Gockeler et al. (QCDSF Collaboration), Phys. Rev. D **71**, 034508 (2005).
[19] J. D. Ashley et al., Eur. Phys. J. A **19**, 9 (2004).
[20] S. F. Pate, Phys. Rev. Lett. **92**, 082002 (2004).
[21] V. Bernard et al., J. Phys. G **28**, R1 (2002).
[22] D. B. Leinweber et al., Phys. Rev. Lett. **94**, 212001 (2005).
[23] D. B. Leinweber et al., Phys. Rev. Lett. **97**, 022001 (2006).
[24] B. W. Filippone and X. D. Ji, Adv. Nucl. Phys. **26**, 1 (2001).
[25] D. Adams et al. [Spin Muon Collaboration (SMC)], Phys. Rev. D **56**, 5330 (1997).
[26] S. L. Zhu et al., Phys. Rev. D **63**, 034002 (2001).
[27] K. S. Kumar and P. A. Souder, Prog. Part. Nucl. Phys. **45**, S333 (2000).